



NRL/MR/6750--04-8747

Design Considerations of a Differentially Pumped Cathode System for LAPPS

DAVID BLACKWELL

SFA, Inc.

Landover, MD

SCOTT G. WALTON

DARRIN LEONHARDT

RICHARD FERNSLER

ROBERT A. MEGER

Charged Particle Physics Branch

Plasma Physics Division

CHRIS MURATORE

ASEE/NRL Postdoctoral Research Associate

February 27, 2004

20040304 058

REPORT DOCUMENTATION PAGE				Form Approved OMB No. 0704-0188	
Public reporting burden for this collection of information is estimated to average 1 hour per response, including the time for reviewing instructions, searching existing data sources, gathering and maintaining the data needed, and completing and reviewing this collection of information. Send comments regarding this burden estimate or any other aspect of this collection of information, including suggestions for reducing this burden to Department of Defense, Washington Headquarters Services, Directorate for Information Operations and Reports (0704-0188), 1215 Jefferson Davis Highway, Suite 1204, Arlington, VA 22202-4302. Respondents should be aware that notwithstanding any other provision of law, no person shall be subject to any penalty for failing to comply with a collection of information if it does not display a currently valid OMB control number. PLEASE DO NOT RETURN YOUR FORM TO THE ABOVE ADDRESS.					
1. REPORT DATE (DD-MM-YYYY) February 27, 2004		2. REPORT TYPE Interim		3. DATES COVERED (From - To)	
4. TITLE AND SUBTITLE Design Considerations of a Differentially Pumped Cathode System for LAPPS				5a. CONTRACT NUMBER	
				5b. GRANT NUMBER	
				5c. PROGRAM ELEMENT NUMBER 67-7641-A4	
				5d. PROJECT NUMBER	
6. AUTHOR(S) David Blackwell,* Scott G. Walton, Chris Muratore,† Darrin Leonhardt, Richard Fernsler, and Robert A. Meger				5e. TASK NUMBER	
				5f. WORK UNIT NUMBER	
7. PERFORMING ORGANIZATION NAME(S) AND ADDRESS(ES) Naval Research Laboratory, Code 6750 4555 Overlook Avenue, SW Washington, DC 20375-5320				8. PERFORMING ORGANIZATION REPORT NUMBER NRL/MR/6750--04-8747	
9. SPONSORING / MONITORING AGENCY NAME(S) AND ADDRESS(ES) Office of Naval Research 800 North Quincy Street Arlington, VA 22217				10. SPONSOR / MONITOR'S ACRONYM(S)	
				11. SPONSOR / MONITOR'S REPORT NUMBER(S)	
12. DISTRIBUTION / AVAILABILITY STATEMENT Approved for public release; distribution is unlimited.					
13. SUPPLEMENTARY NOTES *SFA, Inc., Landover, MD 20785 †ASEE/NRL Postdoctoral Research Associate					
14. ABSTRACT The results of tests of a differential pumping system separating a plasma production cathode chamber and a processing chamber are presented. The tests are a series of measurements taken to evaluate two aspects of system performance. These are the effectiveness of the system to maintain large differential pressures, and, the degree to which different gases in the two chambers can be isolated from one another. It is found that the observed operating range of differential pressure is predicted by the measured conductances and pumping speeds fairly accurately, and the measured conductances themselves are scalable with channel width and pressure in a manner generally consistent with laminar flow. Through the RGA measurements, all three channels tested were found to isolate the cathode from the process chamber gas very well under all except the most egregiously lopsided input flow rates. As the channel is widened, more cathode source gas tends to mix with the process gas and the range of operating pressure becomes more limited. Both of these are alleviated as the pumping speed on the process chamber is increased.					
15. SUBJECT TERMS LAPPS, Plasma processing; Differential pumping					
16. SECURITY CLASSIFICATION OF:			17. LIMITATION OF ABSTRACT UL	18. NUMBER OF PAGES 20	19a. NAME OF RESPONSIBLE PERSON Scott G. Walton
a. REPORT Unclassified	b. ABSTRACT Unclassified	c. THIS PAGE Unclassified			19b. TELEPHONE NUMBER (include area code) (202) 767-7531

CONTENTS

I. INTRODUCTION	1
II. EXPERIMENTAL SETUP	2
III. SYSTEM PARAMETERS	3
IV. DIFFERENTIAL PRESSURE RANGE	6
V. ISOLATION CHARACTERISTICS	7
VI. CONCLUSIONS	9
APPENDIX 1: More on System Parameters	13
APPENDIX 2: Breakdown of Laminar Approximation	14
Acknowledgments	17

Design Considerations of a Differentially Pumped Cathode System for LAPPS

David Blackwell^{*†}, Scott Walton, Chris Muratore[‡],
Darrin Leonhardt, Richard Fernsler, and Robert Meger

U.S. Naval Research Laboratory, Plasma Physics Division Washington, DC

The results of tests of a differential pumping system separating a plasma production cathode chamber and a processing chamber are presented. The tests are a series of measurements taken to evaluate two aspects of system performance. These are the effectiveness of the system to maintain large differential pressures, and, the degree to which different gases in the two chambers can be isolated from one another. It is found that the observed operating range of differential pressure is predicted by the measured conductances and pumping speeds fairly accurately, and the measured conductances themselves are scalable with channel width and pressure in a manner generally consistent with laminar flow. Through residual gas analyzer measurements, all three channels tested were found to isolate the cathode from the process chamber gas very well under all except the most egregiously lopsided input flow rates. As the channel is widened, more cathode source gas tends to mix with the process gas and the range of operating pressure becomes more limited. Both of these effects are alleviated as the pumping speed on the process chamber is increased.

I. INTRODUCTION

Most industrial plasma assisted surface modification applications use highly reactive or even corrosive gases during some stage of the process. Plasmas produced from these gases tend to have large variations in electron density and temperature. There are often multiple ion and neutral species, and the chamber walls and windows can themselves be modified during the processing. Such issues make it very difficult to control the plasma parameters or operate the plasma source under a wide range of conditions. A radiofrequency driven inductive source may have completely different characteristics when the process gas is changed from Cl_2 to CF_4 to SF_6 , for example. At each of these conditions new matching networks and power inputs must be experimentally determined to get an empirical recipe for processing, and even under the most ideal conditions the operator has extremely limited control. Not only is it time consuming and expensive to experimentally go through parameter space to get to a stable operating point, from the scientific standpoint it is difficult to make any headway into the most fundamental questions of plasma processing because of a limited ability to perform controlled experiments.

The LAPPS source is an electron beam driven system which is uniquely qualified to operate as a remote source independent of the process gas pressure and composition. The plasma electrons can be created in one chamber under ideal conditions and shot into the

^{*} Electronic mail: davidb@ccs.nrl.navy.mil

[†] SFA, Inc., Landover, Maryland 20785

[‡] ASEE/NRL Postdoctoral Research Associate

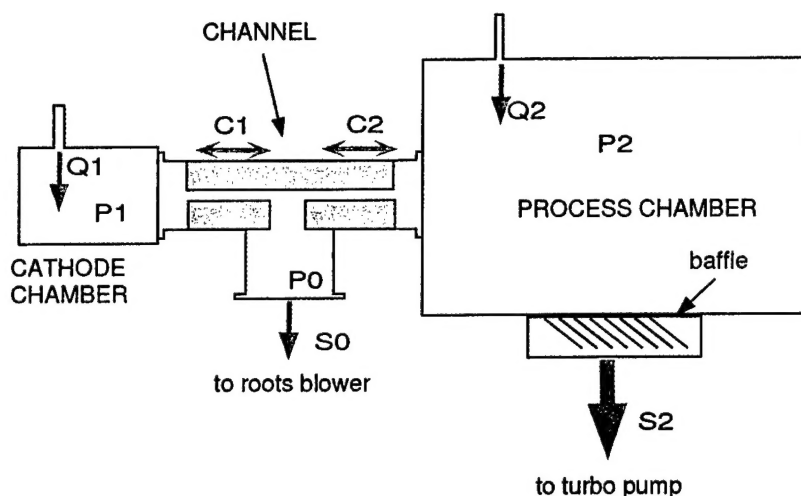


FIG. 1: Experimental setup for differential pumping measurements

process chamber, where the user could set up whatever conditions are required. Multiple step processes utilizing different gases and pressures could be moved through without constant retuning of the source or cleaning of inductive or microwave windows, and a much larger parameter space for processing would be available. To our knowledge, there is currently no source in widespread use that approaches such capabilities.

Achieving such remote operation requires a differential pumping system separating the cathode chamber, where the electron beam is generated from a glow discharge, from the process chamber. In this paper, we test the assumptions of how such a system would operate and examine its effectiveness over a range of conditions.

II. EXPERIMENTAL SETUP

The differential pumping system is a low conductance channel connecting the process chamber and the cathode chamber of the LAPPS plasma source. As shown in figure 1, this channel is pumped on by S_0 , which in this case is a roots pump. Gas is admitted into the two chambers using mass flow controllers Q_1 and Q_2 with a maximum flow rate of 100 sccm each. The turbo pump S_2 has an adjustable baffle at the entrance which can be used to decrease the pumping speed on the process chamber. Measurements of gas pressures P_1 , P_2 , and P_0 are made with a capacitance manometer or convectron tubes. Since there is substantial gas mixing in the channel and process chamber, whenever possible the capacitance manometer is used. The type of gas present in each chamber was measured using a residual gas analyzer (RGA) connected with a low conductance bleed valve. The RGA output is a mass spectrum as shown in figure 2. The most common experimental setup is to flow Argon into the cathode chamber through Q_1 , and the process gas, in this case oxygen, into the process chamber through Q_2 . To average out measurement fluctuations at a particular point in the mass spectrum, the percentage of gas in the spectrum is computed by digitally integrating a width of 1 amu around the mass of the gas of interest, then dividing the result by the entire integrated spectrum.

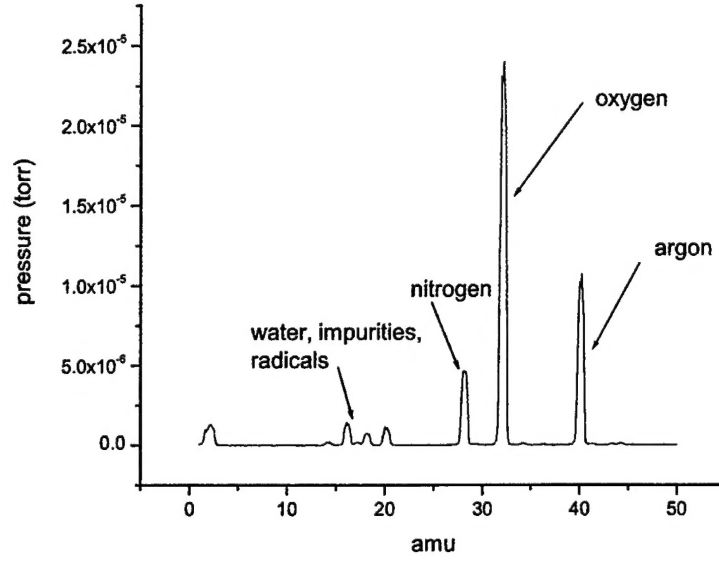


FIG. 2: An example of the output spectrum of the RGA.

III. SYSTEM PARAMETERS

From the setup of the two chambers, the equations governing the system are

$$Q_1 + Q_2 = P_0 S_0 (P_0) + P_2 S_2 (P_2) \quad (1)$$

$$Q_2 = P_2 S_2 (P_2) + C_2 (P_2 - P_0) \quad (2)$$

$$Q_1 = C_1 (P_1 - P_0) \quad (3)$$

with $Q_{1,2}$, $P_{1,2}$, and $C_{1,2}$ the inputs, pressures, and conductances associated with the two chambers, S_2 and S_0 the pumping speeds, and P_0 the pressure at the halfway point between the two chambers. Given any two gas inputs Q_1 and Q_2 and the pumping speeds and conductances, we should be able to predict the pressures P_1 and P_2 , or vice versa. The fact that the pumping speeds are in general functions of the pressure makes these equations nonlinear. In addition, the conductances are also functions of pressure, with the functionality varying depending on what type of flow region we are in.

The flow region is defined by a quantity called the Knudsen number, which is defined as

$$K_n = \frac{\lambda}{d} \quad (4)$$

with λ the mean free path for collisions and d the characteristic dimension of the system. In our case the most critical dimension is the width of the channel. There are only two regions where the channel conductance has analytic expressions. These are the molecular flow region, when $\frac{\lambda}{d} > 1$, and the laminar flow region, where $\frac{\lambda}{d} < 0.01$. Using the approximation

$$\lambda = \frac{5}{P_m \text{ Torr}} \text{ cm} \quad (5)$$

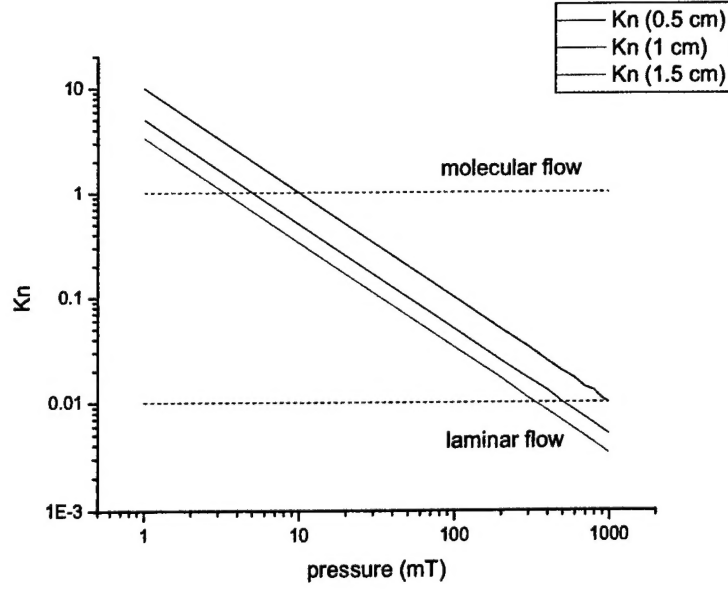


FIG. 3: Knudsen number K_n vs pressure for the three channel widths used in the experiment.

the regions are plotted vs. channel width in figure 3. We can see that almost all pressures typical of LAPPS experiments fall between the molecular and laminar flow regions, where there is no theory to describe the flow or calculate the conductances. These parameters must therefore be determined experimentally.

The conductances are calculated by measuring the pressure drop across the channel vs. the gas input with the turbo pump on the process chamber closed off. When plotted against the mean pressure (figure 4), over a large applicable pressure range the conductance is a linear function of the form

$$C_{1,2} = \alpha \langle P_{1,2}, P_0 \rangle + \beta \quad (6)$$

This is similar in form to the relation given by Williams et al. [1] for the conductance of a rectangular duct of height b , width a , and length l :

$$C \propto Y(b/a) \frac{b^2 a^2}{l} \langle P \rangle \quad (7)$$

with $Y(b/a)$ a linear function defined as

$$Y(b/a) = .87 \frac{b}{a} + .003 \quad (8)$$

for small values of b/a . The measured slopes of the conductances, α , scale very closely to the slopes predicted by this (7) (figure 5). So although the pressure is in range where the flow cannot be quantified as laminar, the conductance vs. changes in pressure, $\alpha \equiv \frac{\Delta C}{\Delta P}$, over different channel heights b , still scales as if we are in laminar flow regime when we widen the channel. Like the conductances, the pumping speeds at the two chambers are also functions of pressure. This is because the pumps themselves do not operate equally well over wide

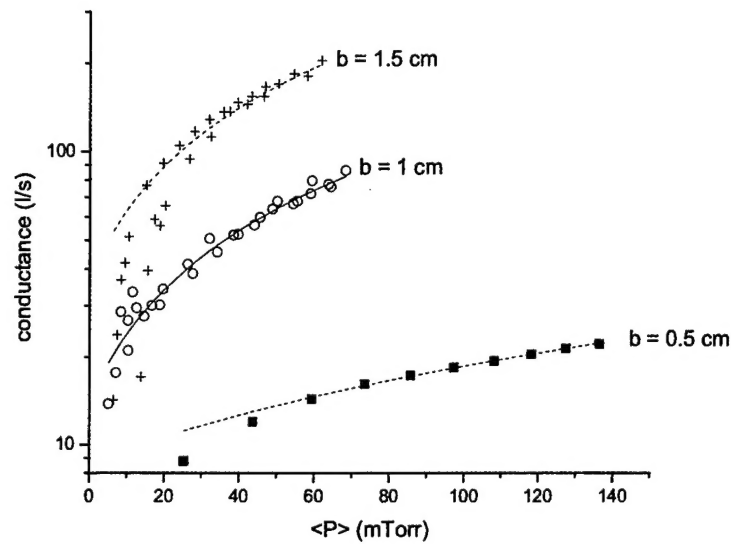


FIG. 4: Channel conductance vs. mean pressure for the three channels.

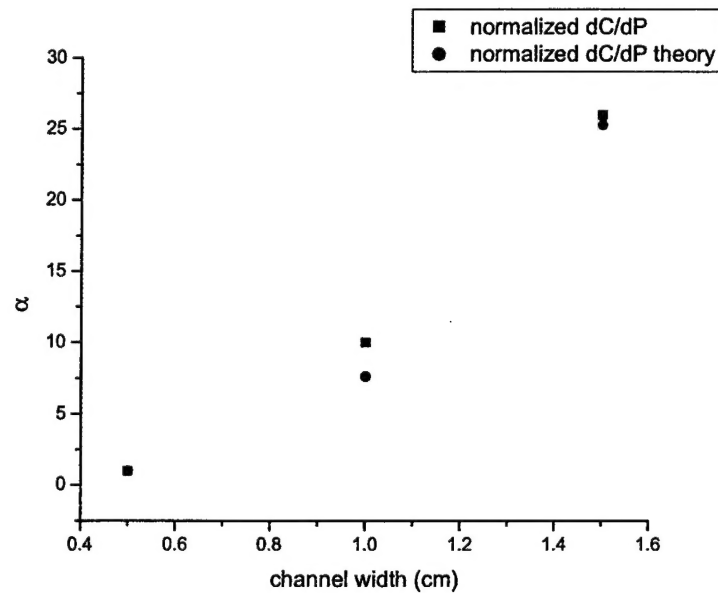


FIG. 5: Slope of the conductance as a function of mean pressure, α , normalized against the slope of the smallest channel.

ranges of pressures, and because the pumps are connected to the system through tubing and baffles which also have pressure dependent conductances. The measured pumping speeds S_0 and S_2 vs. inlet pressure are plotted in figure 6. The turbopump speed S_2 is shown with the baffle in the fully closed position. In this configuration, the pumping speed can be

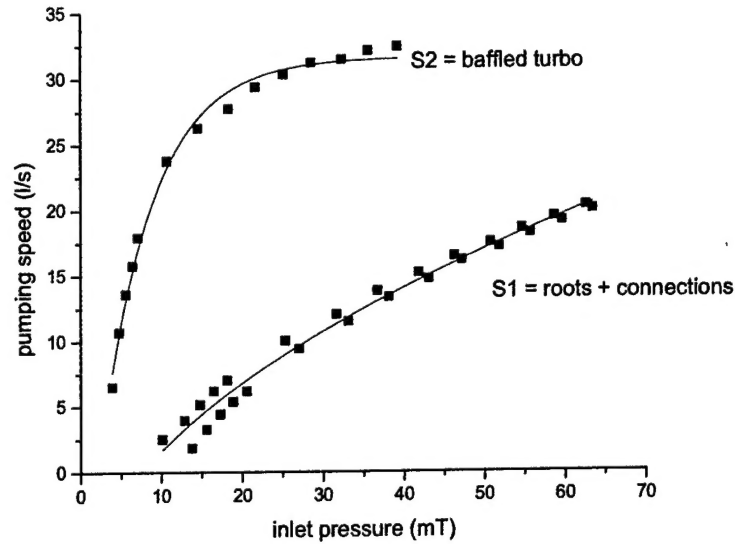


FIG. 6: Effective pumping speeds S_0 and S_2 vs inlet pressure.

expressed as an exponential function:

$$S_2(P_2) = 31.6 - 44e\left(-\frac{P_2}{5.4}\right) \quad (9)$$

with S_2 in l/s and P_2 in mTorr. When the baffle is fully opened, the pumping speed did not vary appreciably from the manufacturer's specifications [2] and was constant over the pressure range tested with a value of 234 l/s with the pump on low speed.

The pumping speed S_0 reflects that of the roots pump combined with the ≈ 1 m of connecting hose. This can be expressed as a square root function:

$$S_0(P_0) = 3.9P_0^{\frac{1}{2}} - 10.9 \quad (10)$$

IV. DIFFERENTIAL PRESSURE RANGE

A useful method of showing the flexibility of the system is to compute bounding curves in pressure space. These are the pressures mapped out when we set either of the gas inputs to zero. These curves give the lower limits of P_1 and P_2 and readily display the range of operating points. This is done by substituting (10), (9), and (6) into (1)-(3) with either Q_1 or Q_2 set to zero, then plugging in gas inputs and solving the system of nonlinear equations iteratively. Every gas input value creates a solution point (P_1, P_2) similar to an x-y coordinate. Multiple values map out a bounding curve in pressure space. Figure 7 (a) and (b) show the bounding curves for the three channels tested with the baffle to the turbopump closed and opened. As expected, the narrowest channel has the widest operating range. It is of interest to observe how the operating range changes with different pumping speeds and conductances. More curves examining this are calculated and discussed in Appendix 1. Using the method described above, we can also compute pressures using experimental values of gas inputs Q_1 and Q_2 . These are plotted along with the measured values in figures 8 -

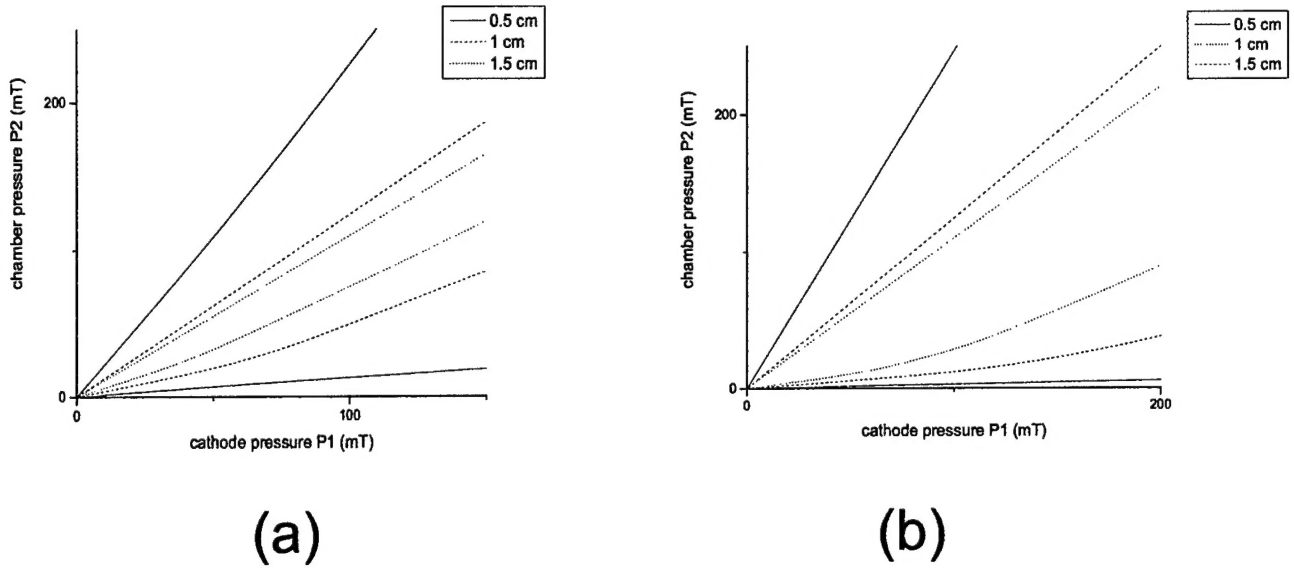


FIG. 7: Bounding curves for the three channels tested with the baffle to the turbopump (a) closed and (b) opened.

10. Defining the error between theory and experiment as the normalized distance between the points in pressure space as

$$error = \sqrt{\frac{(P_{1,ex} - P_{1,th})^2 + (P_{2,ex} - P_{2,th})^2}{(P_{1,ex} + P_{2,ex})^2}} \quad (11)$$

gives us an average error of 25-30% for the three channels. This error is due to slight changes in pumping or conductance curves with argon and oxygen, which were measured using oxygen only. Mixtures of the two gases will have slightly different viscosities. Even with this error, all of the measured points do fall closely within the predicted boundaries.

V. ISOLATION CHARACTERISTICS

In addition to maintaining differential pressure, another important characteristic of the system is the degree to which the gases can be isolated. This can be calculated if we assume that the flow is laminar enough so that gas can only flow in one direction in a channel at a time; i.e., the two gases do not mix in the channels. In such a regime, from (3), any positive value of Q_1 will cause $P_1 > P_0$, so that gas will only flow out of the chamber. Whatever gas is admitted to the process chamber will never reach the cathode chamber. However, gas from the cathode chamber can flow into the process chamber. From (2) we have

$$P_2 S_2(P_2) = Q_2 + C_2 (P_0 - P_2) \quad (12)$$

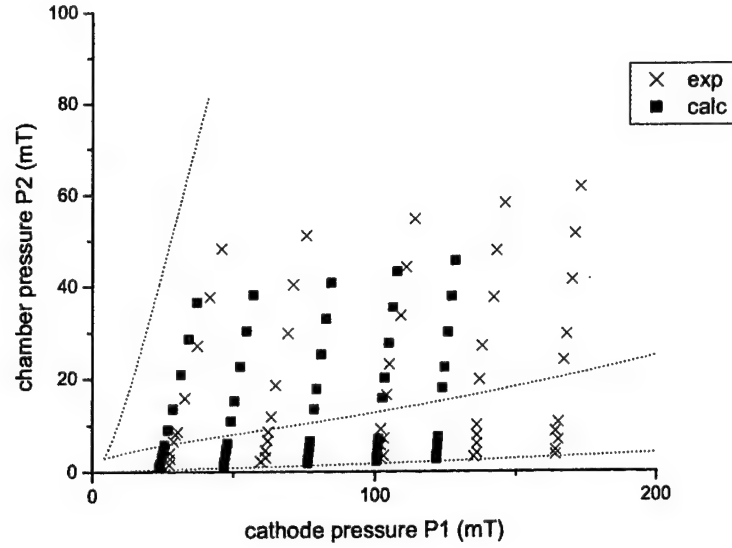


FIG. 8: Measured and calculated values of pressure shown with bounding curves for the 0.5 cm channel.

The first term on the right hand side is the process gas input, while the second term is the gas flowing in from the cathode chamber. In the event that $P_0 < P_2$, gas does not flow from the cathode chamber to the process chamber, and the two chambers are ideally isolated. Again, equations (1)-(3) can be solved iteratively to find the percentage of oxygen in the process chamber for any input condition. The cathode chamber is assumed to have 100% argon. The accuracy of this calculation depends on how well our assumption of laminar flow describes the system.

The percentages of oxygen and argon under each condition (Q_1, Q_2) are computed experimentally by normalizing out all of the other components present due to leaks and impurities, i.e., considering the entire spectrum to be only the two gases we have control over. The percentages of oxygen or argon are then

$$\begin{aligned} \%O_2 &= \frac{\int_w O_2}{\int_w O_2 + \int_w Ar} \\ \%Ar &= \frac{\int_w Ar}{\int_w O_2 + \int_w Ar} \end{aligned} \quad (13)$$

with the integrals being the integrated part of the spectrum 1 amu wide around 40 or 32 amu. Figures 11 - 13 show the fraction of oxygen in the process chamber calculated from the RGA measurements along with the fraction predicted by (1)-(3). The fraction of argon in the cathode chamber from the RGA data is also shown. The plots show that the laminar flow assumption is quite accurate even though theoretically we are not in the laminar regime. Most of the cathode data shows argon percentages above 95%; the average of the median argon percentage is 97% for all three channels with both the baffle opened and closed. The percentage of oxygen varies between 50-75% with a median value of ~60%. The theoretical percentages from the state equation are on average within 15% of the experimental values.

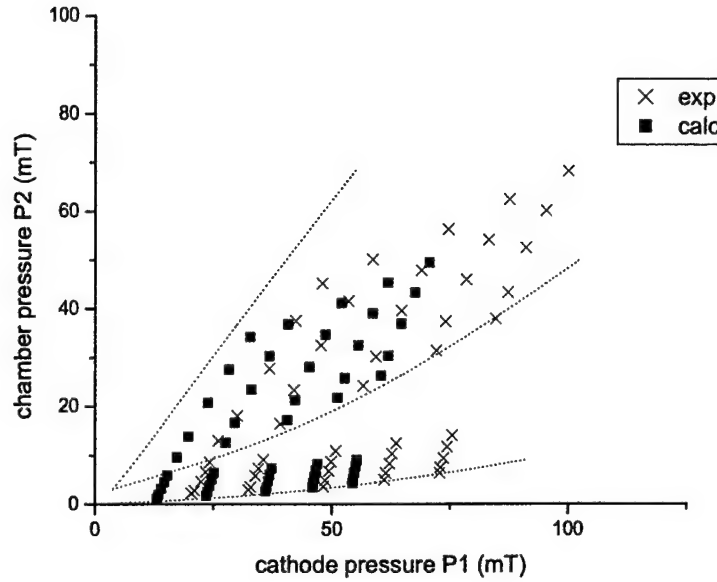


FIG. 9: Measured and calculated values of pressure shown with bounding curves for the 1 cm channel.

This error is somewhat inflated by some theoretical values being greater than unity, when in actuality such answers should be set equal to one. There are some argon percentages in the cathode that are below 90%, indicating a partial breakdown of our assumption; these occur at lower values of $Q_1 + Q_2$, meaning lower gas pressures, or when $Q_2 \gg Q_1$. Increasing S_2 has a negligible effect on the percentages for given inputs, but does expand the range over which we can operate with a high percentage of oxygen in the process chamber. Figures 1414 - 16 show the data points in 2-D pressure space, with a color map to indicate percentages of oxygen. Along with the bounding curves, we have also computed the curve where the process chamber contains equal parts of oxygen and argon, which doesn't necessarily lie exactly between the boundaries. The experimental points can be seen to fall on either side of this curve quite accurately.

VI. CONCLUSIONS

We have tested a differential pumping system to determine range of differential pressure and degree of isolation between two chambers with different input gases. The system was modified by changing the width of the differential channel, and, by changing the speed of the pump on the process chamber by opening and closing the baffle. The conductance and pumping speeds were computed from capacitance manometer pressure readings and known gas inputs from mass flow controllers. The type of gas in the chamber was measured with an RGA, and percentages of process or cathode gas were computed by taking small integrals of the spectrum around the mass points representative of each gas.

It is clear that the narrower channel with an open baffle gives the best range of differential pressure and best isolation. This range shrinks dramatically as the channel is widened, so it is likely that a channel width greater than the largest tested here, 1.5 cm, will have a

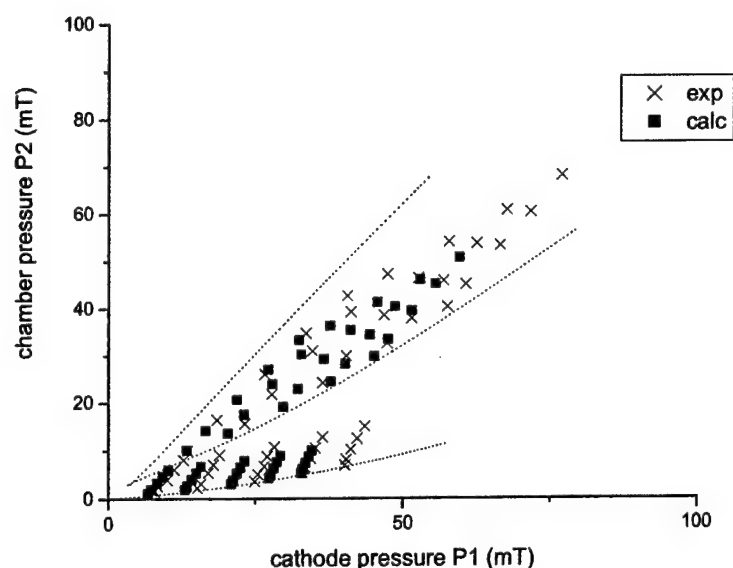
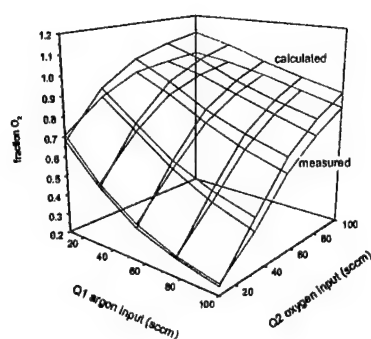
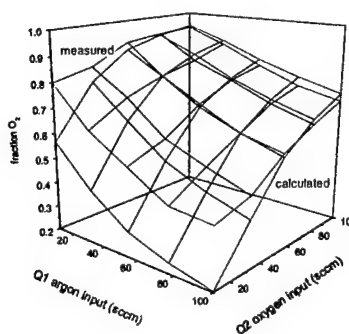


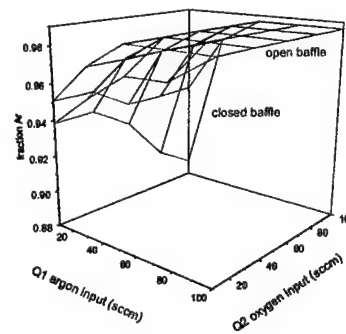
FIG. 10: Measured and calculated values of pressure shown with bounding curves for the 1.5 cm channel.



(a)



(b)



(c)

FIG. 11: (a) The fraction of oxygen in the process chamber calculated from the RGA measurements along with the fraction predicted by (1)-(3) for the 0.5 cm channel. The baffle to the turbopump is closed. (b) Same as (a) but with the baffle opened. (c) The fraction of oxygen in the cathode chamber with the baffle opened and closed.

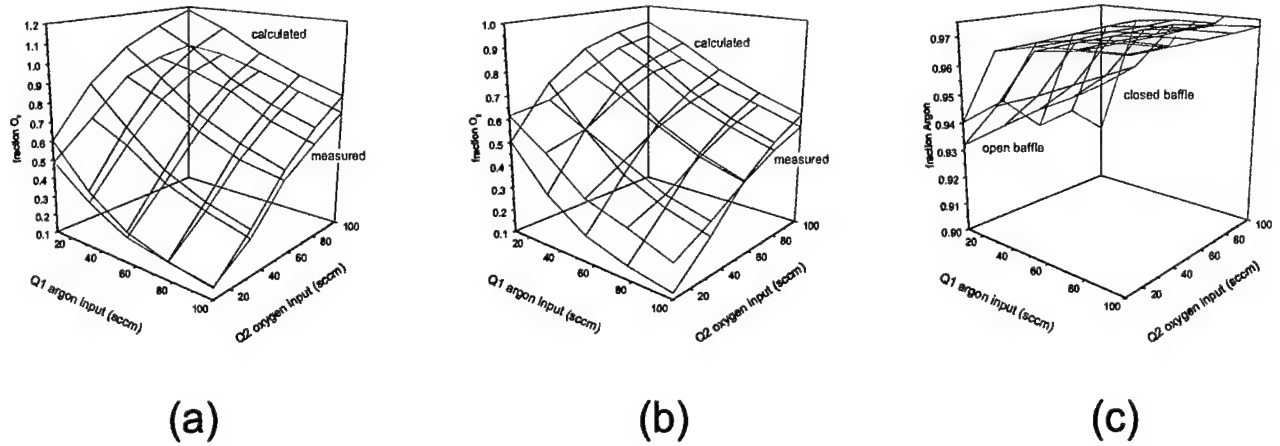


FIG. 12: Same as figure 11 with the channel width increased to 1 cm.

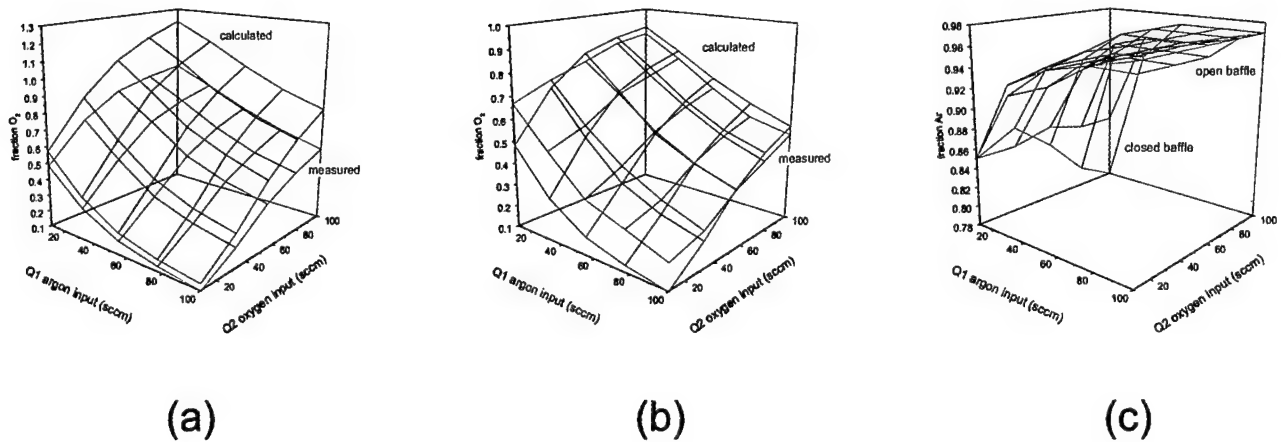


FIG. 13: Same as figure 11 with the channel width increased to 1.5 cm.

severely constrained range of operation. A larger pump on the process chamber will widen this range but also requires a more hardy pump to handle the increased throughput needed to achieve the same pressures.

The cathode was found to be almost ideally isolated from the process chamber under almost all conditions tested; the average percentage of argon was over 95%. The process

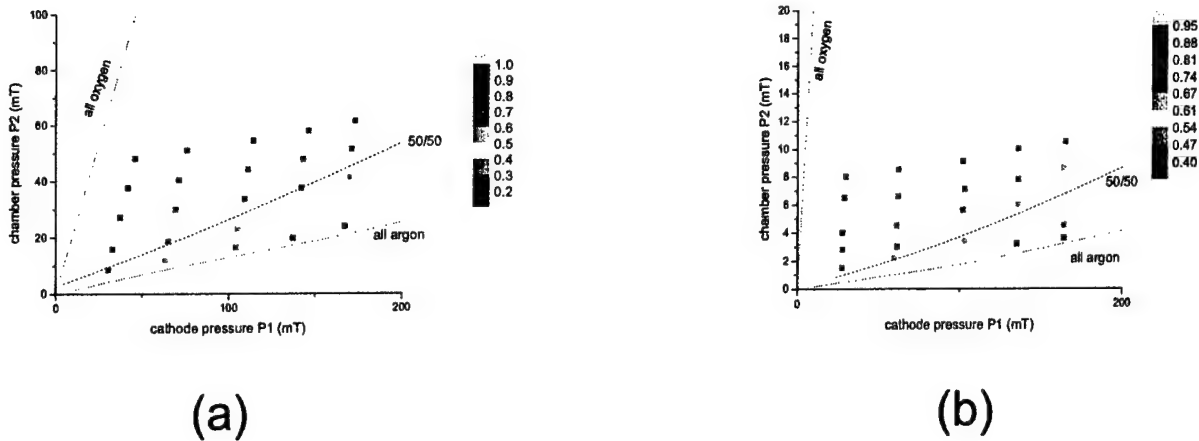


FIG. 14: The percentage of oxygen in the process chamber plotted in pressure space for the 0.5 cm channel. The dashed line between the curves shows the 50% oxygen dividing line; (a) baffle to the turbopump open, (b) baffle closed.

chamber averaged 50-75% oxygen percentage depending on channel width.

Both the range of pressure and the ratio of process to cathode gas can be predicted from the system state equations (1)-(3) if we know the pumping speeds and conductances. The measured conductances do not correspond to formulas from laminar or molecular flow, nor do we expect them to since we are not in either flow region. Experimental fits to these quantities allow us to compute pressures P_1 and P_2 given inputs Q_1 and Q_2 . The computed pressures were found to be within 25-30% of the measured values. This larger error could be due to nonuniformity of the pressure throughout the two chambers, and unaccounted for changes in conductance or pumping speed with different gas mixtures of argon and oxygen. Even with these errors, the experimental points always closely followed the area prescribed by the calculated bounding curves.

Although we are not in the laminar flow regime, some aspects of system operation can be predicted assuming laminar flow. The changes in channel width change the slope of the conductance vs. average pressure curve by almost the same amount that the standard formula from laminar flow does. And, using a laminar flow calculation, the percentage of oxygen in the process chamber is accurate to measured data to within 15%.

From this paper it should be possible to build a similar system, and, by measuring the conductances and pumping speeds predict the amount of oxygen in the process chamber without having to use an RGA. Or, if channels of comparable dimensions are used, one should expect comparable operation to those described here. It also should be possible to predict what effect an increase in pumping speed or decrease in conductance will do to the operation of the system. Some plots and discussion of such parameter changes are in appendix 1.

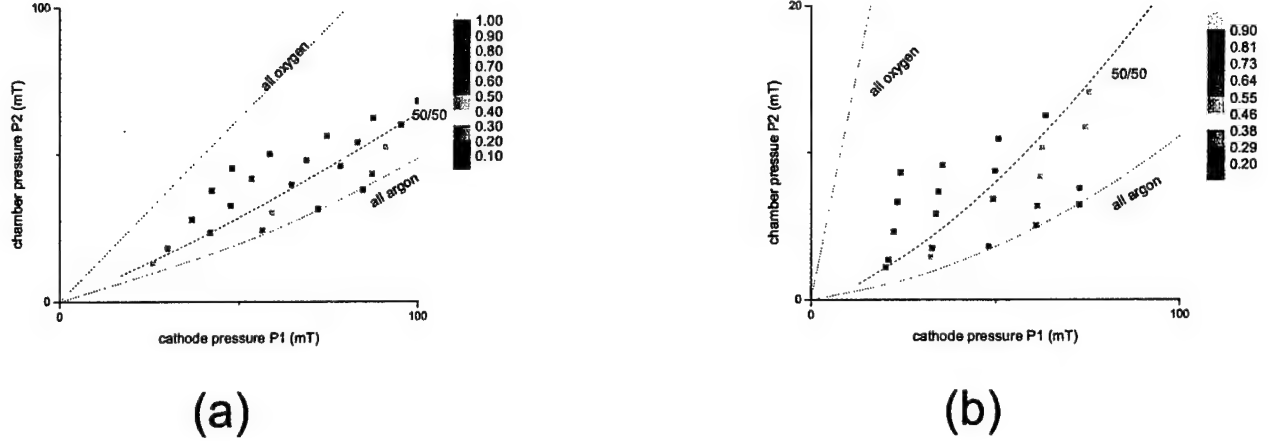


FIG. 15: Same as figure 14 with the channel width increased to 1 cm.

Appendix 1: more on system parameters

There are simple changes that can be made to the system that will improve operation to some degree. These are increasing the pumping speed on the channel or lengthening the channel to increase the conductance. Installing a pump on the cathode chamber would push the bounding curves in figure 7 further apart, thus increasing the differential pressure range, but would come at the expense of greater mixing of the process gas into the cathode. For typical LAPPS operation this would not be an acceptable tradeoff, so such a setup is not considered. We will also consider only the case of the 1.5 cm channel, since this had the most limited operating range of the three tested.

Let us first calculate what happens as we increase the pump speed S_0 . If we could for example double the pump speed by upgrading to the next most powerful roots blower, we can iteratively solve equations (1)-(3) to calculate new bounding curves. Figure 17 shows that the region of operation is only slightly expanded when such a change is made. However, upgrading S_0 to a 150 l/s turbo pump has a much greater effect, as shown in figure 18. This type of result is expected; the upper and lower curves represent P_2 in terms of P_1 when either Q_1 or Q_2 is set to zero. These give the equations

$$P_2 = \frac{C_2 + S_0}{C_2} P_1 \quad (14)$$

for the upper bounding curve, and

$$P_2 = \frac{C_1 P_1}{(S_0 + C_1) \left(\frac{C_2 + S_2}{C_2} \right) + S_2} \quad (15)$$

for the lower curve. These equations are nonlinear because the pumping speeds and conductances are themselves functions of P_1 and P_2 , but we can still get an idea of how the system

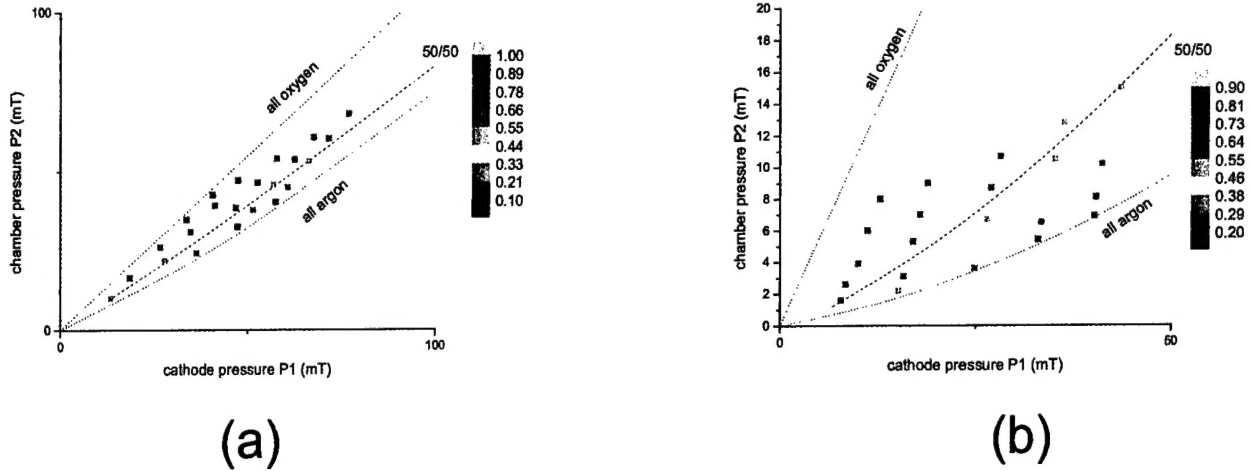


FIG. 16: Same as figure 14 with the channel width increased to 1.5 cm.

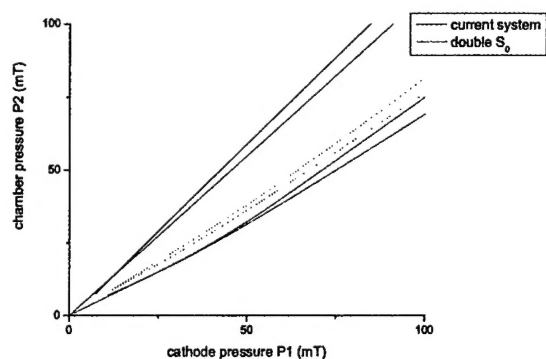
behaves. The channel pump term S_0 always appears with one of the conductances, so to have an appreciable effect the pumping speed should be comparable to those values. This channel typically has a conductance of more than 100 l/s, which is already twice as large as the manufacturer's specified pumping speed of the roots blower without any connecting pipes or tubing. Notice also that the upper bounding curve is nearly independent of S_2 , which was observed experimentally as well. An alternative to changing the pump could be to decrease the channel conductance by increasing its length. Figure 19 shows the new bounding curves computed for this change. The lower curve is pushed downward appreciably, but the upper bounding curve, being a weaker function of the conductance, is expanded much less.

From these calculations we can see that significant improvement in the operation of the differential pumping system can be obtained with a substantial increase in channel pump speed. Lengthening the channel also improves the operation by allowing higher ratios of P_1 to P_2 , and, to a much lesser extent, higher ratios of P_2 to P_1 .

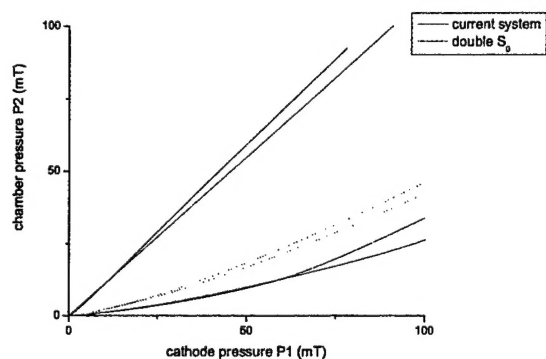
Appendix 2: breakdown of laminar approximation

Under most circumstances the laminar approximation that the cathode is nearly 100% argon is a good way of computing the oxygen percentage in the process chamber. However, there were some experimental conditions when the argon percentage was only in the 80's; these were for the 1 cm and 1.5 cm channels when $Q_2 \gg Q_1$. Under such conditions the assumption that gas only flows in one direction in each channel is no longer valid, and the cathode becomes contaminated with process gas.

To examine this, we substituted a needle valve for the mass flow controller so that Q_2 could be increased higher than 100 sccm. With no argon input, and the baffle closed,

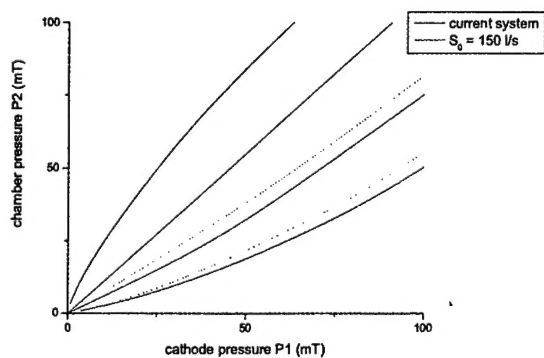


(a)

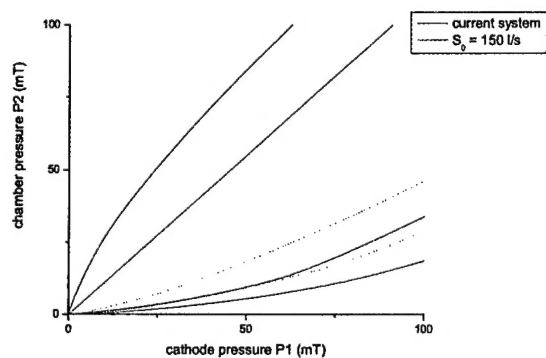


(b)

FIG. 17: The effect of doubling the channel pump (roots blower) pumping speed S_0 on the 1.5 cm channel bounding curves in pressure space with the turbopump baffle (a) closed and (b) open.

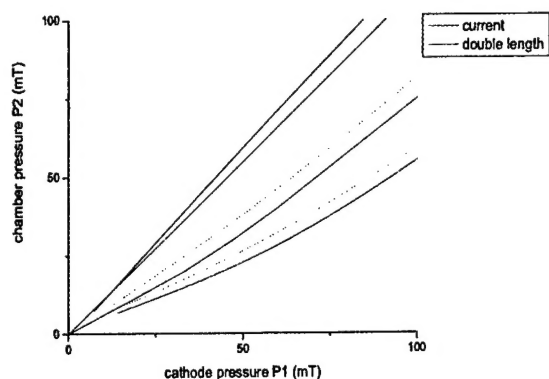


(a)

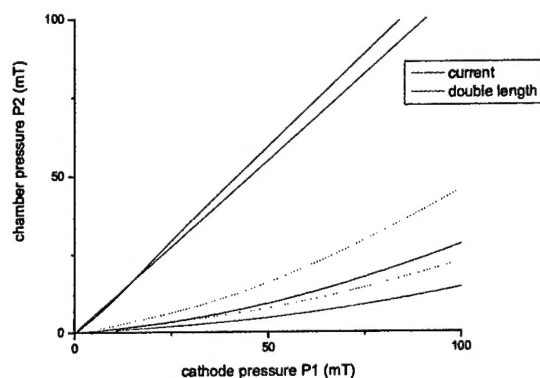


(b)

FIG. 18: The same as figure 17, this time with a 150 l/s turbopump substituted for the roots blower.

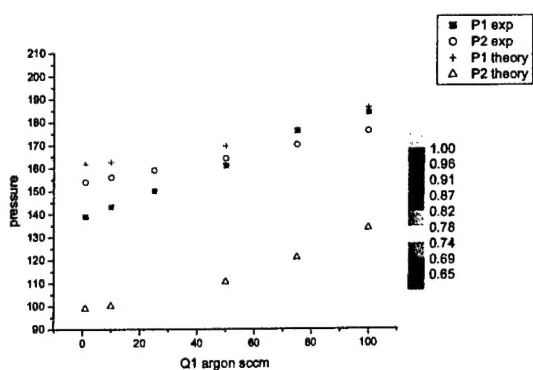


(a)

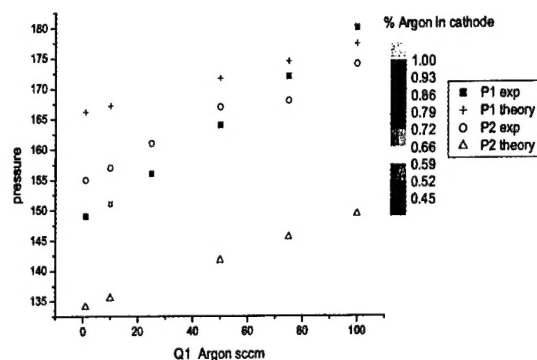


(b)

FIG. 19: As in figure 17; the effect of doubling the channel length while leaving the roots blower constant.



(a)



(b)

FIG. 20: High pressure breakdown of the laminar flow assumption. At sufficiently large Q_2 with respect to Q_1 , the cathode chamber can become contaminated with process gas. (a) 1 cm channel, (b) 1.5 cm channel.

the process chamber pressure was set to ≈ 150 mT. This corresponded to $Q_2 \approx 720$ -750 sccm. The amount of argon admitted to the cathode chamber was incrementally increased. Figure 20 shows the measured and experimental gas pressures in each chamber with the argon percentage in the cathode chamber (the oxygen percentage in the process chamber measured 100% for all data points). Under some conditions we can see that the amount of oxygen in the cathode chamber is quite high; as large as 40-50% of the total. However, in both the 1 cm and 1.5 cm channel one we get to around $Q_1 \approx 75$ sccm argon, only one tenth the value of Q_2 , the percentage of argon in the cathode is over 90%.

Thus, at points in pressure space near the upper bounding curve where $Q_2 \gg Q_1$ the argon percentage in the cathode can drop to less than acceptable levels. Fortunately, such conditions are rare in normal processing applications.

Acknowledgments

The Office of Naval Research supported this work.

-
- [1] J.F. O' Hanlon, *A Users Guide to Vacuum Technology, second edition*, p.31, John Wiley & Sons, 1989
 - [2] Leybold Product and Vacuum Technology Reference Book